Star Clusters: From the Milky Way to the Early Universe
Proceedings IAU Symposium No. 351, 2019
A. Bragaglia, M. Davies, A. Sills & E. Vesperini, eds.

doi:10.1017/S1743921319008202

An empirical clock to measure the dynamical age of star clusters

Francesco R. Ferraro

Dipartimento di Fisica e Astronomia, Università degli Studi di Bologna,
Via Gobetti 93/2, I–40129 Bologna, Italy
email: francesco.ferraro3@unibo.it

Abstract. The observational properties of a special class of stars (the so-called Blue Straggler stars - BSSs) in Globular Clusters are discussed in the framework of using this stellar population as probe of the dynamical processes occurring in high-density stellar systems. In particular, the shape of the BSS radial distribution and their level of central segregation have been found to be powerful tracers of the level of the dynamical evolution of the hosting cluster, thus allowing the definition of an empirical chronometer able to measure the dynamical age of star clusters.

Keywords. blue stragglers, globular clusters, techniques: photometric

1. Introduction

Globular clusters (GCs) are populous and dense stellar systems. They are among the few cosmic structures that within the timescale of the age of the Universe, can possibly undergo nearly all the physical processes known in stellar dynamics (energy equipartition, mass segregation, dynamical friction, core collapse). Indeed, gravitational interactions among stars significantly alter the overall energy budget of the parent cluster with a dramatic effect on its internal dynamical evolution. This dynamical activity has been suggested to promote the formation of stellar exotica, like interacting binaries, blue stragglers and millisecond pulsars (Bailyn (1995); Pooley *et al.* (2003); Ransom *et al.* (2005)).

Blue Straggler stars (BSSs) surely are the most famous and numerous population of exotic objects known in star clusters. In the color-magnitude diagram (CMD) of a stellar cluster, they are easily distinguishable from normal stars since they define a sort of sequence extending brighter and bluer than the main sequence (MS) turn-off (TO) point (e.g., Sandage (1953); Ferraro *et al.* (1992, 1993, 1997a, 2003); Leigh *et al.* (2007); Moretti *et al.* (2008); Simunovic & Puzia (2016); Parada *et al.* (2016)). The details of their formation mechanism is not completely understood yet, although it is widely accepted that they are hydrogen-burning stars more massive than the MS-TO objects (Shara *et al.* (1997); Gilliland *et al.* (1998)). Since any recent star formation event can be realistically ruled out in GCs, two main mechanisms are commonly advocated to explain their origin: (1) mass-transfer (MT) in binary systems McCrea (1964) possibly up to the complete coalescence of the two stars, and (2) direct stellar collisions (COLL; Hills & Day (1976)). The efficiency of both these processes depends on the local environment (Fusi Pecci *et al.* (1992); Ferraro *et al.* (1999, 2006a); Davies *et al.* (2004); Dalessandro *et al.* (2008b); Sollima *et al.* (2008); Knigge *et al.* (2009)), and they can act simultaneously within the same cluster (Ferraro *et al.* (2009); Xin *et al.* (2015); Dalessandro *et al.* (2013a); Beccari *et al.* (2019)).

Independently on their formation mechanism, BSSs represent a population of heavy objects ($M_{BSS} = 1.0 - 1.4 M_{\odot}$, Fiorentino *et al.* (2014); Raso *et al.* (2019)) orbiting in

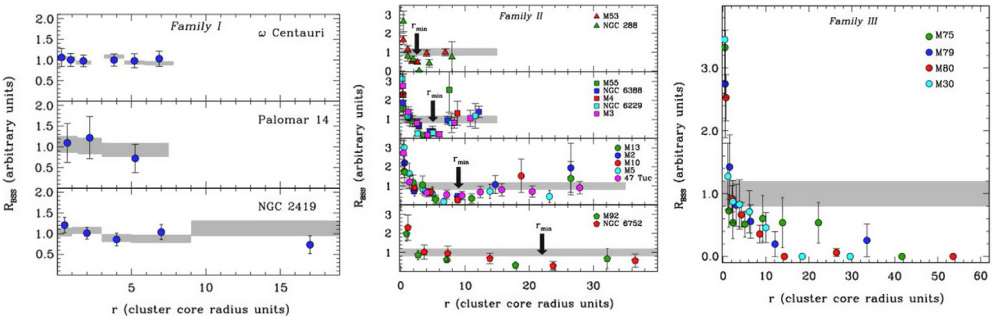

Figure 1. Normalized radial distribution of BSSs (colored symbols) compared to that of normal cluster stars taken as reference (grey regions) in the three main families defined by Ferraro *et al.* (2012): *Family I* = dynamically young clusters (left panel), *Family II* = dynamically intermediate-age clusters (central panel), *Family III* = dynamically old clusters (right panel).

a sea of lighter stars (the average stellar mass in an old GC is $< M >= 0.33 M_{\odot}$). For this reason BSSs can be used as powerful gravitational probe particles to investigate key physical processes (such as mass segregation and dynamical friction) characterizing the dynamical evolution of star clusters (e.g., Ferraro *et al.* (2009, 2012); Dalessandro *et al.* (2013a); Simunovic *et al.* (2014)). Conversely, the signature of these processes imprinted in the BSS observational features can be used to trace the dynamical history of the parent cluster. This is the core concept of the dynamical clock (see Ferraro *et al.* (2012); Lanzoni *et al.* (2016); Ferraro *et al.* (2018)).

2. Defining the "dynamical clock"

Ferraro *et al.* (2012) analysed the BSSs radial distribution over the entire extension in a sample of 21 Galactic GCs (Ferraro *et al.* (1997a, 2004, 2006a); Sabbi *et al.* (2004); Lanzoni *et al.* (2007a,b,c); Dalessandro *et al.* (2008a,b, 2009); Beccari *et al.* (2006a,b, 2011); Contreras Ramos *et al.* (2012); Sanna *et al.* (2012)) and first demonstrated that the shape of the BSS radial distribution can be used to measure the level of dynamical evolution reached by the host system. In doing this they used the "BSS normalized radial distribution" (hereafter BSS-nRD), defined as the ratio between the fraction of BSSs sampled in a radial bin and the fraction of cluster light sampled in the same bin (Ferraro *et al.* (1993)). Thus, the analysed sample of chronologically old and coeval GCs have been grouped in three main families on the basis of the shape of their BSS-nRD (see Fig. 1):

- Family I, for which the BSS-nRD is flat (i.e. the radial distribution of BSSs within the cluster is fully compatible with that of the sampled light);
- Family II, for which the BSS-nRD is bimodal (with a high peak in the cluster center, a dip at an intermediate radius $r_{\rm min}$, and a rising branch in the external regions);
- Family III, for which the BSS-nRD shows only a central peak followed by a monotonically decreasing trend.

Since BSSs have masses larger than normal cluster stars, these behaviours have been interpreted as the manifestation of the dynamical friction, which drives the objects more massive than the average toward the cluster centre, with an efficiency that mainly depends on the local star density (i.e. it decreases for increasing radial distance). Hence, a flat BSS-nRD indicates that dynamical friction has not affected the BSS population (not even in the innermost regions) and therefore Family I clusters are "dynamically young" (see left paneles in Fig. 1). In more evolved clusters (Family II), dynamical friction has been more and more efficient, affecting regions at increasingly larger distances from

https://doi.org/10.1017/S1743921319008202 Published online by Cambridge University Press

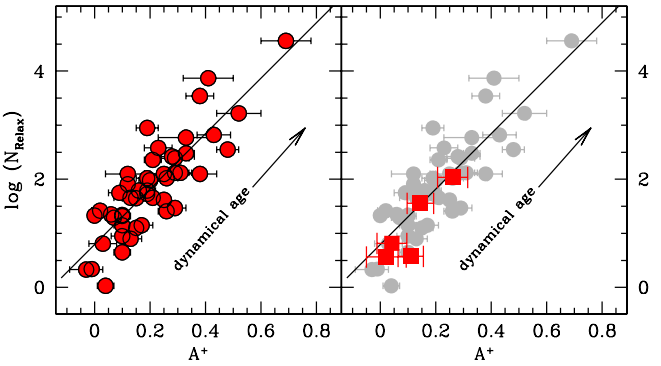

Figure 2. *Left Panel:* Relation between A^+ and N_{relax} (which quantifies the number of current central relaxation times occurred since cluster formation) for the sample of 48 Galactic GCs discussed in Ferraro *et al.* (2018). The tight relation between these two parameters (solid line) demonstrates that the segregation level of BSSs can be efficiently used to evaluate the level of dynamical evolution experienced by the parent cluster. *Right Panel:* The same as in the left panel (with the sample of Galactic GCs shown in grey) with the five LMC clusters discussed in Ferraro *et al.* (2019) highlighted as red squares.The LMC clusters ranked at increasing value of the dynamical age are NGC1841, Hodge 11, NGC2257, NGC1466 and NGC2210.

the center, as marked by the observed position of $r_{\rm min}$ (see central paneles in Fig. 1). In "dynamically old" systems the dynamical friction affected also the most remote BSSs, thus producing a monotonic BSS-nRD with a central peak only (Family III, right panel in Fig. 1).

In spite of many and independent observational confirmations (Li *et al.* (2013); Beccari *et al.* (2013); Dalessandro *et al.* (2013b); Sanna *et al.* (2014); Singh & Yadav (2019)), the current generation of N-body and Monte Carlo simulations of GCs seems yet unable to reproduce the details of the BSS-nRD evolution, possibly indicating a still insufficient level of realism (Miocchi *et al.* (2015); Hypki & Giersz (2017); Sollima & Ferraro (2019)). On the other hand, due to its own definition, $r_{\rm min}$ is located in a region of "low signal", where dynamical friction is removing heavy stars and the number of BSSs reaches its minimum (the so called "zone of avoidance"; Mapelli *et al.* (2004, 2006)). Thus we searched for additional and "more easily detectable" observables able to describe the BSS segregation process.

In Alessandrini *et al.* (2016) a new parameter (A^+) to measure the level of BSS central sedimentation, was proposed. The parameter is defined as the area enclosed between the cumulative radial distribution of BSSs and that of a reference (lighter) population, measured within a given distance from the cluster center (the half-mass radius). N-body simulations demonstrate that this parameter increases significantly as a function of time, following the dynamical evolution of the cluster and, more specifically, tracking the process of BSS segregation (see Figure 5 in Alessandrini *et al.* (2016)). At initial times, when all stars are spatially perfectly mixed regardless of their mass, BSSs and the REF population have the same cumulative radial distributions and $A^+ = 0$. As mass segregation proceeds, BSSs migrate toward the centre of the system and the two curves start to separate, thus providing a progressively increasing value of the A^+ parameter. Lanzoni *et al.* (2016) measured the new parameter within one half-mass radius (A^+_{rh}) for the same set of clusters discussed in Ferraro *et al.* (2012), finding a tight correlation with $r_{\rm min}$ (see their Figure 2). This relation demonstrates that they both the parameters measure the effect of the dynamical friction in progressively centrally segregating BSSs. In fact as clusters get dynamically older, the dynamical friction progressively removes BSSs at increasingly larger distances from the center (thus generating a minimum at increasingly larger

https://doi.org/10.1017/S1743921319008202 Published online by Cambridge University Press

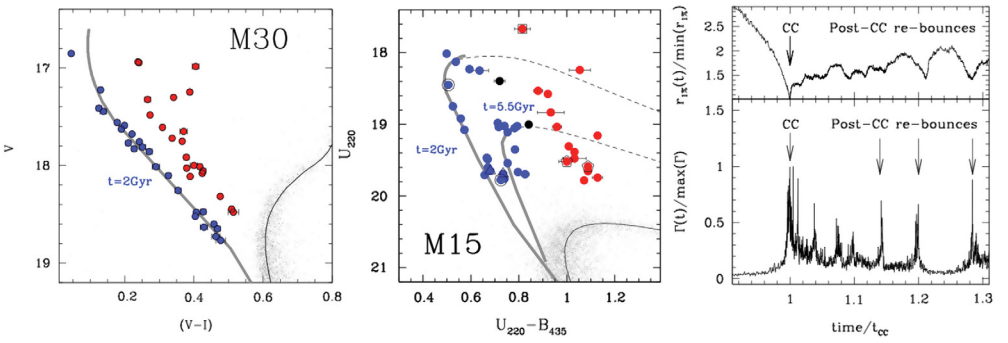

Figure 3. *Left Panel:* The double BSS sequence in M30 (from Ferraro *et al.* (2009)). The thick-line is the 2 Gyr collisional isochrone from Sills *et al.* (2009). *Central Panel:* The double BSS sequence in M15 (from Beccari *et al.* (2019). Two branches are apparent along the blue sequence they are reproduced by a 2 Gyr-old and a 5.5 Gyr-old collisional isochrone, respectively.*Right Panel:* The evolution in time of the 1% Lagrangian radius (top panel) and of the collisional parameter (bottom panel). The 'Core Collapse (CC) epoch and the main Post-CC re-bounces are indicated by the arrows.

values of $r_{\rm min}$) and accumulates them toward the cluster center (thus increasing A^+). In addition, Lanzoni *et al.* (2016) found a strong correlation between A^+ and the central relaxation time of the cluster (t_{rc}) (similar to that found by Ferraro *et al.* (2012) using the parameter $r_{\rm min}$), thus fully confirming that A^+ can be efficiently used to measure the level of dynamical evolution reached by the star cluster.

Ferraro *et al.* (2018) used the large dataset acquired within the HST UV Legacy Survey of Galactic Globular Clusters (Piotto *et al.* (2015), see also Raso *et al.* (2017)) to extend this approach to a sample of 48 GCs. A strong correlation (see left panel of Figure 2) was found between A^+ and the number of relaxation times occurred since cluster formation (computed as $N_{relax} = t_{GC}/t_{rc}$, where $t_{GC} = 12$ Gyr is the average age of the GCs in the sample (Forbes & Bridges (2010)).

The "dynamical clock" has been recently used by Li *et al.* (2019) to measure the dynamical age of 7 intermediate-age (between 700 Myr and 7 Gyr) clusters in the Large Magellanic Cloud (LMC) finding a low-level of dynamical evolution. Interesting enough, instead Ferraro *et al.* (2019) measured the BSS segregation level in five old LMC GCs (with ages comparable to Galactic GCs) detecting clear-cut differences in their level of dynamical evolution (see the right panel of Figure 2). The figure also shows the impressive matching with the trend defined by the Galactic GCs (grey circles), demonstrating that the "dynamical clock" can be efficiently used in any stellar environment. In addition Ferraro *et al.* (2019) found that the five studied LMC GCs nicely followed the tight correlation between the dynamical age and the size of the core found by Ferraro *et al.* (2018) for the Galactic clusters, thus confirming that the long-term dynamical evolution tends to generate compact objects. This result proposes a new reading of the long-standing age-size distribution in the LMC clusters in terms of the long-term cluster internal dynamical evolution (Ferraro *et al.* (2019)).

3. Exploring the Post Core Collapse (PCC) phase

The BSS observational features might also provide crucial information about the most spectacular dynamical event in the cluster lifetime: the collapse of the core. This branch of the research was initiated by the discovery by Ferraro *et al.* (2009) of two well-separated and almost parallel sequences of BSSs in the post-core collapse (PCC) cluster M30 (left panel in Figure 3). This was the very first time that such a feature was detected

https://doi.org/10.1017/S1743921319008202 Published online by Cambridge University Press

in any stellar system and it opened the possibility to distinguish between the two BSS formation processes. In fact, the comparison with evolutionary models of BSSs formed by direct collisions of two MS stars (Sills *et al.* (2009)) showed that the blue-BSS sequence is well fit by collisional isochrones with ages of ∼2 Gyr. Instead, the red-BSS population is far too red to be reproduced by collisional isochrones of any age, and it turned out to be compatible with the portion of the CMD where MT binary models are expected (Xin *et al.* (2015), see also recent models by Jiang *et al.* (2017) showing that MT-BSS might also "contaminate" the blue-BSS sequence). However the impressive agreement of the blue-BSS with the COLL isochrones suggests that the vast majority of these stars have a collisional origin and they are nearly co-eval possibly *generated by short-lived event* (the Core Collapse - CC). On the other hand the extension of the blue sequence and the existence of the gap suggest that this was a relatively *recent* event. In fact, due to standard stellar evolution, in a few Gyrs the progeny of blue-BSSs will populate the region between the two observed sequences, thus filling fill the gap. On the basis of these considerations, Ferraro *et al.* (2009) concluded that *most of BSSs along the blue sequence formed simultaneously (during the CC) and the extension in luminosity of this sequence dates the occurrence of this event back to 1–2 Gyr ago.*

Indeed this scenario was recently fully confirmed by Portegies Zwart (2019) who presented detailed stellar merger simulations for this cluster, concluding that the blue population formed in a burst that started ∼3.2 Gyr ago with a peak-rate formation of 30 BSS/Gyr and a time-scale of 0.93 Gyr, possibly triggered by the cluster CC while the red sequence formed at a constant rate of ∼2.8 BSSs/Gyr over the last 10 Gyr.

Recently Beccari *et al.* (2019) discovered a double BSS sequence in the center of the PCC cluster M15 (see the central panel in Fig. 3).† Also in this case the red sequence cannot be reproduced by COLL isochrones of any ages, but this time the blue sequence showed a much more complex structure. In fact two branches are distinguishable: the first branch appears extremely narrow, it extends up to 2.5 mag brighter than the cluster main-sequence turnoff (MS-TO) point, and it is nicely reproduced by a 2 Gyr-old collisional isochrone. The second branch extends up to 1.5 mag from the MS-TO and it is reproduced by a 5.5-Gyr old collisional isochrone Beccari *et al.* (2019) interpreted these features as the observational signature of two major collisional episodes suffered by M15, likely connected to the collapse of its core: the first one (possibly tracing the beginning of the CC process) occurred approximately 5.5 Gyr ago, while the most recent one (possibly associated with a core oscillation in the post-CC evolution) dates back to ∼2 Gyr ago. This scenario is consistent with results from Monte Carlo simulations. The right panel of Figure 3 describes the time evolution of the 1% Lagrangian radius (top panel) and of the collisional parameter (bottom panel) for a cluster reaching the CC and undergoing core oscillations. As shown, the initial deep CC (clearly distinguishable at $t/t_{CC} = 1$) leads to the largest increase in the value of the collisional parameter (Γ), and it is followed by several distinct re-collapse episodes leading to secondary peaks of the Γ parameter. Thus the BSS populations observed along the two branches of the blue-BSS sequence in M15 might be produced during the initial main collapse and during one of the subsequent collapse events, sufficiently intense to trigger a significant number of COLL-BSS production.

These results provides strong evidence supporting the deep connection between the BSS properties and globular cluster dynamical evolution, also opening new perspectives on the study of CC and post-CC evolution.

† Interestingly, the double BSS feature has been detected also in two additional clusters: NGC 362 (Dalessandro *et al.* (2013a)) and NGC 1261 (Simunovic *et al.* (2014)), while the case of the intermediate-age cluster in the LMC NGC2173 is still debated since the feature can possibly be due to the contamination of the LMC field (see Li *et al.* (2018a,b); Dalessandro *et al.* (2019a,b)).

https://doi.org/10.1017/S1743921319008202 Published online by Cambridge University Press

References

Alessandrini, E., Lanzoni, B., Miocchi, Ferraro, F. R., & Vesperini, E. 2016, *ApJ*, 833, 252
Bailyn, C. D. 1995, *ARA&A*, 33, 133
Beccari, G., Ferraro, F. R., Possenti, A., *et al.* 2006, *AJ*, 131, 2551
Beccari, G., Ferraro, F. R., Lanzoni, B., & Bellazzini, M. 2006, *ApJ* (Letters), 652, L121
Beccari, G., Sollima, A., Ferraro, F. R., *et al.* 2011, *ApJ* (Letters), L3
Beccari, G., Ferraro, F.R., Dalessandro, E., *et al.* 2019, *ApJ*, 876, 87
Beccari, G., Dalessandro, E., Lanzoni, B., *et al.* 2013, *ApJ*, 776, 60
Contreras Ramos, R., Ferraro, F. R., Dalessandro, E., *et al.* 2012, *ApJ*, 748, 91
Dalessandro, E., Lanzoni, B., Ferraro, F. R. *et al.* 2008a, *ApJ*, 677, 1069
Dalessandro, E., Lanzoni, B., Ferraro, F. R. *et al.* 2008b, *ApJ*, 681, 311
Dalessandro, E., Beccari, G., Lanzoni, B., *et al.* 2009, *ApJSS*, 182, 509
Dalessandro, E., Ferraro, F. R., Massari, D., *et al.* 2013a, *ApJ*, 778, 135
Dalessandro, E., Ferraro, F. R., Lanzoni, B., *et al.* 2013b, *ApJ*, 770, 45
Dalessandro, E., Ferraro, F. R., Bastian, N., *et al.* 2019a, *A&A*, 621, A45
Dalessandro, E., Ferraro, F. R., Bastian, N., *et al.* 2019b, *Research Notes of the American Astronomical Society*, 3, 38
Davies, M. B., Piotto, G., & de Angeli, F. 2004, *MNRAS*, 349, 129–134
Djorgovski, S. & King, I. R. 1986, *ApJ* (Letters), 305, L61
Djorgovski, S. 1993, in: S. G. Djorgovski & G. Meylan (eds) *Structure and Dynamics of Globular Clusters* (San Francisco: Astronomical Society of Pacific), p. 373
Ferraro, F. R., Fusi Pecci, F., & Buonanno, R. 1992, *MNRAS*, 256, 376
Ferraro, F. R., Fusi Pecci, F., Cacciari, C., *et al.* 1993, *AJ*, 106, 2324
Ferraro, F. R., Paltrinieri, B., Fusi Pecci, F., *et al.* 1997a, *A&A*, 324, 915
Ferraro, F. R., Paltrinieri, B., Fusi Pecci, F., *et al.* 1997b, *ApJ* (Letters), 484, L145
Ferraro, F. R., Paltrinieri, B., Rood, R. T., & Dorman, B. 1999, *ApJ*, 522, 983
Ferraro, F. R., D'Amico, N., Possenti, A., Mignani, R. P., & Paltrinieri, B. 2001. *ApJ*, 561, 337
Ferraro, F. R., Sills, A., Rood, R. T., Paltrinieri, B., & Buonanno, R. 2003, *ApJ*, 588, 464
Ferraro, F. R., Beccari, G., Rood, R. T., Bellazzini, M., Sills, A., & Sabbi, E. 2004, *ApJ*, 603, 127
Ferraro, F. R., Sollima, A., Rood, R. T., *et al.* 2006a, *ApJ*, 638, 433
Ferraro, F. R., Sabbi, E., Gratton, R., *et al.* 2006b, *ApJ* (Letters), 647, L53
Ferraro, F. R., Beccari, G., Dalessandro, E., *et al.* 2009, *Nature*, 462, 1028
Ferraro, F. R., Lanzoni, B., Dalessandro, E., *et al.* 2012, *Nature*, 492, 393
Ferraro, F. R., Lapenna, E., Mucciarelli, A., *et al.* 2016, *ApJ*, 816, 70
Ferraro, F. R.,Lanzoni, B., Raso, S., *et al.* 2018, *ApJ*, 860, 36
Ferraro, F. R.,Lanzoni, B., Dalessandro, E., *et al.* 2019, *Nat. Astr.*, 3, 1149
Fiorentino, G., Lanzoni, B., Dalessandro, E., *et al.* 2014, *ApJ*, 783, 34
Forbes, D. & Bridhes, T. 2010, *MNRAS*, 404, 1203
Fusi Pecci, F., Ferraro, F. R., Corsi, C. E., Cacciari, C., & Buonanno, R. 1992, *AJ*, 104, 1831
Gilliland, R. L., Bono, G., Edmonds, P. D., *et al.* 1998, *ApJ*, 507, 818
Hills, J. G. & Day, C. A. 1976, *ApJ* (Letters), 17, L87
Hypki, A. & Giersz, M. 2017, *MNRAS*, 471, 2537
Jiang, D., Chen, X., Li,L., & Han, Z. 2017, *ApJ*, 849, 100
Knigge, C., Leigh, N., & Sills, A. 2009, *Nature*, 457, 288
Lanzoni, B., Sanna, N., Ferraro, F. R., *et al.* 2007a, *ApJ*, 663, 1040
Lanzoni, B., Dalessandro, E., Ferraro, F. R., *et al.* 2007b, *ApJ*, 663, 267
Lanzoni, B., Dalessandro, E., Ferraro, F. R., *et al.* 2007c, *ApJ* (Letters), 668, L139
Lanzoni, B., Ferraro, F. R., Alessandrini, E. *et al.* 2016, *ApJ*, 833, L29
Leigh, N., Sills, A., & Knigge, C. 2007, *ApJ*, 661, 210
Leigh, N., Knigge, C., Sills, A., *et al.* 2013, *MNRAS*, 428, 897
Li, C., de Grijs, R., Deng, L., & Liu, X. 2013, *ApJ* (Letters), 770, L7
Li, C., Deng, L., de Grijs, R., Jiang, D., & Xin, Y. 2018, *ApJ*, 856, 25
Li, C., Deng, L., de Grijs, R., Jiang, D., & Xin, Y. 2018, *Research Notes of the American Astronomical Society*, 2, 215

Li, C., Sun, W., Hong, J., *et al.* 2019, *ApJ*, 871, 171
Mapelli, M., Sigurdsson, S., Colpi, M., *et al.* 2004, *ApJ* (Letters), 605, L29
Mapelli, M., Sigurdsson, S., Ferraro, F. R., *et al.* 2006, *MNRAS* 373, 361
McCrea, W. H. 1964, *MNRAS*, 128, 147
Meylan, G. & Heggie, D. C. 1997. *ARA&A*, 8, 1
Miocchi, P., Lanzoni, B., Ferraro, F. R. *et al.* 2013, *ApJ*, 774, 151
Miocchi, P., Pasquato, M., Lanzoni, B., *et al.* 2015, *ApJ*, 799, 44
Moretti, A., de Angeli, F., & Piotto, G. 2008, *A&A*, 483, 183
Parada, J., Richer, H., Heyl, J. *et al.* 2016, *ApJ* 830, 139
Pietrinferni, A., Cassisi, S., Salaris, M., & Castelli, F. 2006, *ApJ* 642, 797
Piotto, G., De Angeli, F., King, I. R. *et al.* 2004, *ApJ* (Letters), 604, L109
Piotto, G., Milone, A. P., Bedin, L. R., *et al.* 2015, *AJ* 149, 91
Pooley, D., Lewin, W. H. G., Anderson, S. F., *et al.* 2003, *ApJ* (Letters), 591, L131
Portegies Zwart, S. 2019, *A&A* 621, 10
Ransom, S. M., Hessels, J. W. T., Stairs, I. H., *et al.* 2005, *Science*, 307, 892
Raso, S., Ferraro, F.R., Dalessandro, E. *et al.* 2017, *ApJ*, 839, 64
Raso, S., Pallanca, C., Ferraro, F.R., *et al.* 2019, *ApJ*, ...
Sandage A. R. 1953, *AJ* 58, 61.
Sabbi, E., Ferraro, F. R., Sills, A., *et al.* 2004, *ApJ*, 617, 1296
Sanna, N., Dalessandro, E., Lanzoni, B., *et al.* 2012, *MNRAS* 422, 1171
Sanna, N., Dalessandro, E., Ferraro, F. R., *et al.* 2014, *ApJ*, 780, 90
Shara, M. M., Saffer, R. A., & Livio, M. 1997, *ApJ* (Letters), 489, L59
Sills, A., Karakas, A., & Lattanzio, J. 2009, *ApJ*, 692, 1411
Simunovic, M., Puzia, T. H., & Sills, A. 2014, *ApJ* (Letters), 795, L10
Simunovic, M. & Puzia, T. H. 2016, *MNRAS*, 462, 3401
Singh, G. & Yadav, R. K.S. 2019, *MNRAS*, 482, 4874
Sollima, A., Lanzoni, B., Beccari, G., Ferraro, F. R., & Fusi Pecci, F. 2008, *A&A*, 481, 701
Sollima, A. & Ferraro, F. R. 2019, *MNRAS*, 483, 1523
Tian, B., Deng, L.-C., Han, Z.-W., & Zhang, X.-B. 2006. *A&A*, 455, 247
Xin, Y., Ferraro, F. R., Lu, P., *et al.* 2015, *ApJ*, 801, 67

https://doi.org/10.1017/S1743921319008202 Published online by Cambridge University Press